Available online at www.sciencedirect.com

ScienceDirect

Procedia Structural Integrity 68 (2025) 472–479

Structural Integrity Procedia

www.elsevier.com/locate/procedia

European Conference on Fracture 2024

A New Design for Mitigating Interfering Modes in Cruciform Specimens to Enhance Ultrasonic Fatigue Testing

Diogo Montalvão[a,*], Sina Safari[b], Weston Chidzikwe[a], Phil Sewell[a], Pedro Costa[c,d], Luís Reis[c], Manuel Freitas[c,d]

[a] *ADDISONIC, Department of Design and Engineering, Bournemouth University, Poole BH12 5BB, UK*
[b] *School of Electrical, Electronic and Mechanical Engineering, University of Bristol, Queen's Building, University Walk, Bristol BS8 1TR*
[c] *IDMEC, Instituto Superior Técnico, Universidade de Lisboa, Av. Rovisco Pais, 1, 1050-099 Lisboa, Portugal*
[d] *Universidade Atlântica, Instituto Universitário, Fábrica de Pólvora de Barcarena, 2730-036 Barcarena, Portugal*

Abstract

Cruciform specimens have been extensively used to simulate biaxial loading conditions in Ultrasonic Fatigue Testing (UFT), particularly within the Very High Cycle Fatigue (VHCF) regime. However, these specimens are often affected by interference from unintended flexural modes, such as the 'flapping mode,' which occur at frequencies near the desired axial mode, compromising the accuracy and reliability of the tests. To address this issue, a new specimen design has been developed to effectively separate the axial and flexural modes, thereby transforming the precision of fatigue testing. Finite Element Analysis (FEA) and experimental validation using Digital Image Correlation (DIC) were employed to optimise the geometry of the specimens, resulting in a substantial frequency separation between the interfering flexural modes and the axial mode. Through this redesign, mode coupling has been virtually eliminated, ensuring that the specimens deform as intended during testing. This breakthrough enables in-plane biaxial testing across the full range of biaxiality ratios, overcoming the previous challenges posed by mode coupling. Equibiaxial in-phase biaxial UFT with this type of cruciform specimen, previously considered largely theoretical in its practical application, has now been successfully realised through the innovations presented in this work.

Peer-review under responsibility of ECF24 organizers

Keywords: Ultrasonic Fatigue Testing; Very High Cycle Fatigue; Multiaxial Loads; Modal Analysis.

* Corresponding author. Tel.: +44 01202 965 513.
E-mail address: dmontalvao@bournemouth.ac.uk

Peer-review under responsibility of ECF24 organizers
10.1016/j.prostr.2025.06.084

1. Introduction

As demand grows for resource-efficient designs in industrial applications while maintaining safety standards, predicting the mechanical behaviour of load-bearing parts becomes crucial, especially in industries such as automotive, marine, medical, robotics, and aerospace. This is particularly true for materials subjected to cyclic loads and fatigue, where accurate life prediction is essential, especially for new alloys like Titanium, Inconel, or those produced via Metal Additive Manufacturing (MAM). MAM parts, with heterogeneous microstructures, lack readily available fatigue data, such as S-N curves, unlike conventional alloys. While traditional alloys were once thought to have a fatigue limit beyond 10^7 cycles, it is now known that materials do not have infinite life, requiring testing up to 10^8, 10^9, or more cycles (Bathias 1999), known as Very High Cycle Fatigue (VHCF).

VHCF testing is challenging and impractical using slower machines such as rotating bending at 30 Hz due to the time and cost involved. Ultrasonic Fatigue Testing (UFT) machines, generally operating at 20 kHz (Furuya et al. 2022), have made testing in this regime feasible, achieving 10^9 cycles theoretically in 14 hours, though intermittent cooling extends the time to 3–4 days — still a major improvement over conventional methods (Costa et al. 2020).

While most fatigue testing remains uniaxial, multiaxial stresses are more common in real-world structures, making biaxial testing more representative. Biaxial testing is particularly important for anisotropic materials like rolled metal sheets or MAM components. Uniaxial test results often do not adequately characterise multiaxial loading, where failure can occur at lower stress levels. Initial biaxial fatigue testing focused on tension-torsion or in-plane biaxial conditions (Freitas 2017). Recent studies (Costa et al. 2020) have demonstrated that UFT machines can achieve biaxial cyclic loading conditions, even in the VHCF regime.

For in-plane biaxial testing, cruciform test specimens allow for varying biaxiality ratios, from B=1 (equibiaxial tension-tension, T-T) to B=-1 (pure shear, compression-tension, C-T), passing through B=0 (uniaxial, Poisson's ratio ν=0) (Montalvão et al. 2019, Costa et al. 2020). However, issues have arisen with equibiaxial specimens, where a specific flexural 'flapping mode' interferes with the intended axial deformation, due to the close proximity of the axial and flapping mode frequencies (2.5% difference, as shown by Costa et al., 2019).

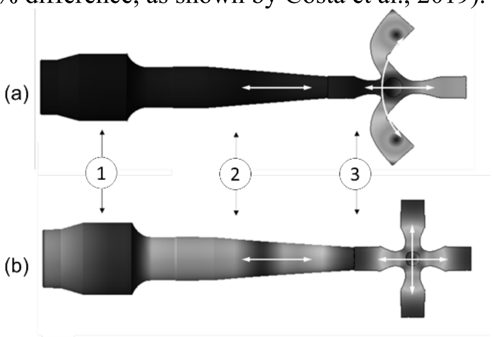

Fig. 1. FEA simulation results as in Costa et al. (2019) showing the deformation of the (a) equibiaxial mode shape at 20 kHz and the (b) 'flapping' mode shape at 20.5 kHz, where 1 is the booster, 2 is the horn and 3 is the non-modified version of a T-T specimen.

In this study, a novel T-T cruciform specimen design is introduced. This new design shifts the resonant frequency of the flexural mode away from the axial mode, ensuring that the axial mode dominates during testing while minimising interference from other mode shapes. Finite Element Analysis (FEA) was employed for the optimisation of the geometry, and Digital Image Correlation (DIC) was used to experimentally validate the findings. Additionally, the study addresses transient mode issues and proposes refinements to improve the system operation. These contributions represent a significant advancement in the accuracy and reliability of UFT, ensuring more precise stress and strain measurements, which are crucial for enabling accelerated fatigue testing through UFT. Equibiaxial in-phase biaxial (T-T) UFT with this type of cruciform specimen, previously regarded as theoretically possible but impractical, has now been successfully achieved through the innovations presented in this work.

2. Proposed design principles

2.1. Explanation of the 'flapping' mode shape issue

Consider the example of an arbitrary 3 Degree-Of-Freedom (DOF) system, i.e., one that has 3 mode shapes and corresponding natural frequencies. The Frequency Response Function (FRF) of such system is given by:

$$H(\omega) = \sum_{r=1}^{3} \frac{\bar{A}_r}{\omega_r^2 - \omega^2 + i\eta_r\omega_r^2} \tag{1}$$

where $\bar{A}_r$ is the complex modal constant of mode r, ω_r is the angular natural frequency, ω is the angular operational frequency, η_r is the hysteretic modal damping ratio, and $i = \sqrt{-1}$. As an example, it is assumed that modes 1, 2 and 3 have the following resonant frequencies, respectively: $f_1 = 20\ kHz$, $f_2 = 20.5\ kHz$ and $f_3 = 25\ kHz$. It is further assumed that all modal constants and hysteretic damping rations are identical across all modes, i.e., $\bar{A}_1 = \bar{A}_2 = \bar{A}_3 = 1 + i$ and $\eta_1 = \eta_2 = \eta_3 = 0.02$. Under these conditions, the graphical representation of equation (1) is shown in Fig. 2 (a).

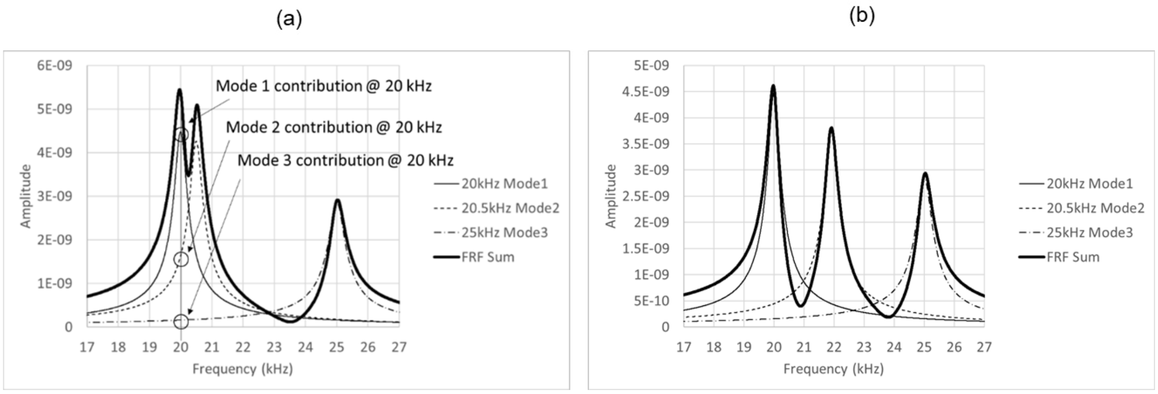

Fig. 2. (a) Amplitude of the FRF of an arbitrary 3 DOF system with frequencies 20 kHz, 20.5 kHz and 25 kHz; (b) amplitude of the FRF of an arbitrary 3 DOF system with frequencies 20 kHz, 21.9 kHz and 25 kHz.

Fig. 2 (a) shows that, at the 20 kHz operational frequency (mode 1), the system experiences significant contributions from mode 2, despite its 20.5 kHz resonant frequency. This is evident as the FRF sum (bold line) is larger than mode 1 alone (narrow line), indicating the system vibrates with a combination of both modes, introducing bending. In the cruciform specimen, mode 1 corresponds to the biaxial mode, while mode 2 represents the 'flapping' mode. Mode 3 shows that sufficiently spaced modes have negligible impact. As Costa et al. (2019) demonstrated, the 'flapping' mode causes overheating at the specimen-horn connection and prevents the maximum stress from occurring at the centre as intended.

2.2. Principles of shifting the frequency of the 'flapping' mode shape 'away'

Although cruciform specimens have complex geometry, their thicker tips and thinner centre allow for a helpful analogy: they can be viewed as four intersecting massless beams with concentrated masses at the tips, as shown in Fig. 3.

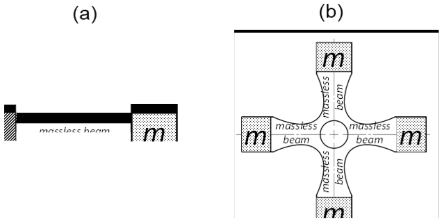

Fig. 3. Idealised representation of the cruciform specimen: (a) model of a cantilever massless beam with a concentrated mass at the tip; (b) analogy of the cruciform specimen to a system composed of four intersecting massless beams with concentrated masses at tips.

The natural frequencies of a massless beam with a concentrated mass m at its tip are given by:

$$f_{axial} = \frac{1}{2\pi}\sqrt{\frac{AE}{mL}} \tag{2}$$

$$f_{bending} = \frac{1}{2\pi}\sqrt{\frac{EI}{mL^3}} \tag{3}$$

for axial and bending mode shapes, respectively, where A is the area of the cross section, E is the Young's modulus and L is the length of the beam. If the tip mass is moved closer to the centre by shortening the beam, $f_{bending}$ will increase by a factor raised to the power of 3 compared to f_{axial} (since L is raised to 1/2 in equation (2) and 3/2 in equation (3)). The mass must then be proportionally increased to maintain the axial mode at 20 kHz, but as the mass affects both frequencies equally, shortening the beam while increasing the tip mass will inevitably raise $f_{bending}$.

2.3. Adaptation of the design principles into cruciform UFT specimens

The principles were applied to the T-T specimen in Fig. 1 and 4 (a), resulting in the design shown in Fig. 4 (b). Based on the work of Baptista et al. (2015) and refined by Montalvão and Wren (2017) and Montalvão et al. (2019), the new design retains key features, such as elliptical corners (1), concave thickness reduction at the centre (2), and the M6 mounting thread (3). However, the tips' thickness (4) was increased by 4 mm in total (2 mm per side). This added thickness can be integrated into the original design or retrofitted as glued overtips. Fig. 4 (b) shows that the modified specimen is 11.7% shorter.

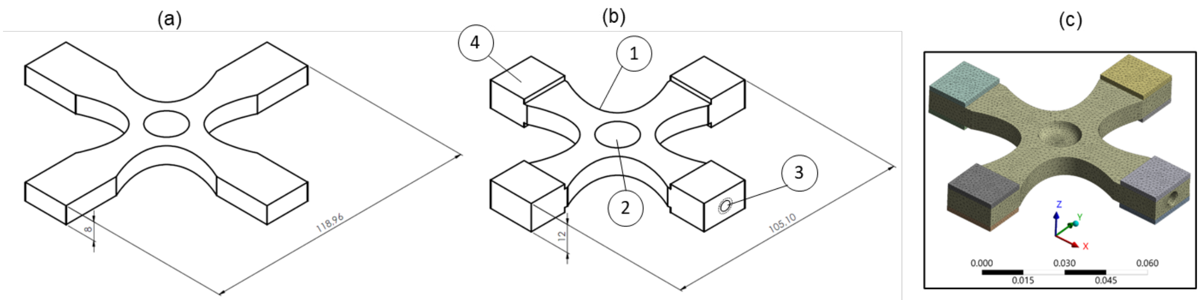

Fig. 4. Comparison between T-T specimens before and after the new design principles are implemented: (a) original design; (b) design with added overtips; (c) mesh of the design with added overtips in the FEA packageANSYS (dimensions in mm).

Considering the analogy of a 3 DOF system, with modes 1 and 3 remaining at 20 kHz and 25 kHz, and mode 2 shifting from 20.5 kHz to 21.9 kHz, Fig. 2 (a) becomes Fig. 2 (b). At 20 kHz, the sum aligns with mode 1, indicating that contributions from modes 2 (the 'flapping' mode) and 3 are negligible. As a result, the specimen now performs as intended at 20 kHz due to the design modifications.

3. Materials and Methods

3.1. Modal and harmonic computational simulations

FEA was employed to analyse the modal behaviour of Aluminium (Al) 6082-T6 cruciform specimens. ANSYS 2023 R2 was used to model the new design (Fig. 4 (c)). The principle guiding the redesign was that reducing the arm length would increase the flexural frequency by a factor of 3/2 relative to the axial frequency. It is important to mention that the computational model included both the horn and the specimen so that the simulation would replicate the actual physical system as close as possible. Harmonic response analysis further confirmed that the axial mode remained dominant at 20 kHz, with minimal contributions from other modes.

3.2. Experimental testing

The experiments were conducted in the ADDISONIC lab at Bournemouth University (Fig. 5) as part of the effort to mitigate interfering modes in cruciform specimens used in UFT. A combination of FEA, point measurements with LASER sensors from Keyence, and DIC from DANTEC, were employed to validate the deformation patterns in the specimens. The goal was to ensure that the axial mode was dominant at the operating frequency of 20 kHz, while minimising the interference from nearby modes, particularly the flapping mode. DIC is a non-contact optical method used to measure full-field displacements and strains on the surface of the specimen. With high-speed sampling frequencies up to 125 kHz, the system allowed capturing a series of images of the specimen during deformation at 20 kHz. Pixel pattern changes allowed calculation of strain distributions at the centre of the specimen.

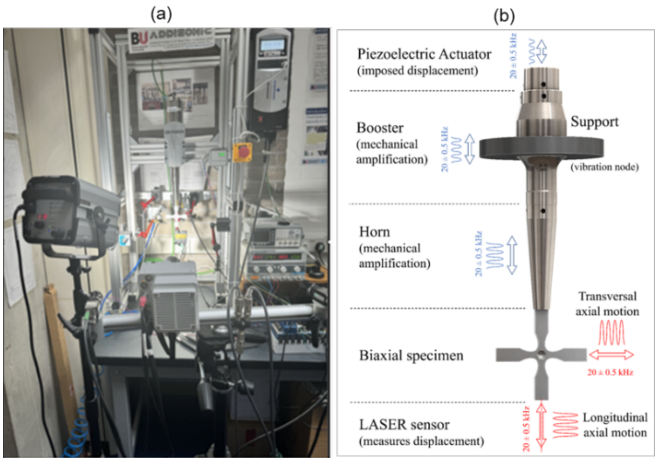

Fig. 5. (a) experimental setup in the ADDISONIC lab at Bournemouth University; (b) schematic of the setup as per Montalvão and Wren (2017).

4. Results

4.1. Modal and harmonic computational simulations

The modal and harmonic analysis performed on the stack with the specimen demonstrated significant separation between the axial and flapping modes. FEA simulations confirmed that the modified specimen successfully shifted the flapping mode frequency from 20.5 kHz to 22.7 kHz, providing a frequency gap greater than 10% (Fig. 6), i.e., it allowed mitigating the interference of the flapping mode shape through creating sufficient separation from the axial mode at ~20 kHz. This gap reduced the coupling of these modes, ensuring that the specimen will primarily deform in the axial mode during testing, validating the hypothesis from Costa et al. 2019.

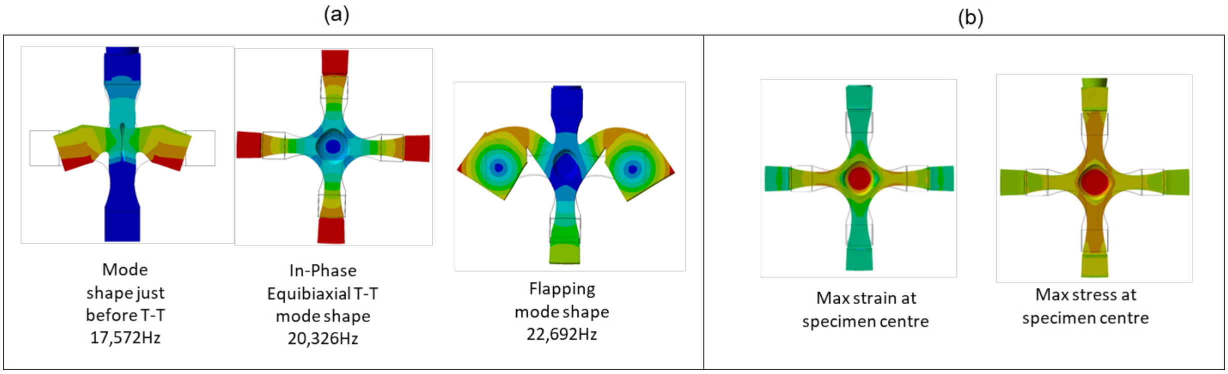

Fig. 6. (a) deformation results from the modal analysis in ANSYS with modes immediately before and immediately after the intended mode shape; (b) strain and stress results from the harmonic analysis in ANSYS at the 20.3 kHz resonating frequency.

4.2. Experimental results

DIC analysis provided validation of FEA, showing a strong correlation between the simulated and experimental strain distributions. The maximum stress and strain remained at the centre of the specimen, as predicted. DIC analysis showed that maximum stress and strain occurred at the centre of the specimen (Fig. 8), as intended, and the strain distribution was consistent with the FEA predictions. However, despite the strong correlation between FEA and LASER and DIC measurements, there were still some initial discrepancies. Transient modes detected during testing resulted in local deviations from the expected strain patterns, particularly near the edges of the specimen (Fig. 6 (b)). These disturbances were likely caused by slight asymmetries in the mounting setup and boundary conditions. Introducing beeswax between the horn and specimen, along with a slight reduction in the length of the threaded connection to ensure a flush fit, effectively reduced these issues. This is shown in Fig. 7, where measurements taken perpendicular to the arms (a) display a mode shape with high amplitude at approximately 3.3 kHz (b, c, and d), which disappears (e) after the specimen-horn connection was corrected.

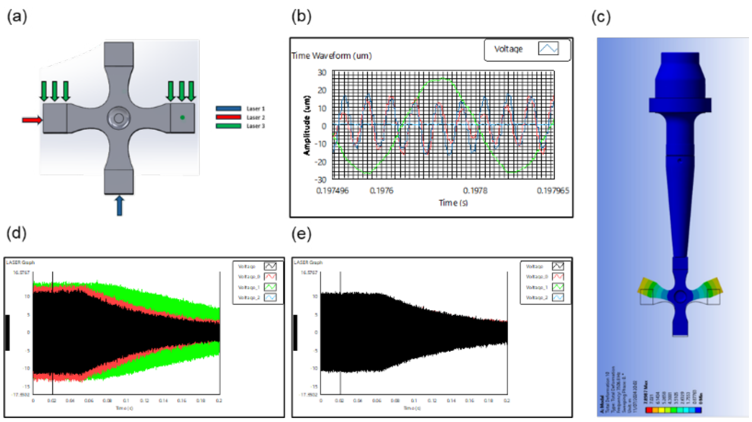

Fig. 7. (a) Schematic of LASER measurement locations; (b) displacement waveforms from 3 LASERS during steady state; (c) FEA model of a mode shape at ~3.3 kHz; (d, e) transient system responses during coast down, before and after fixing the connection.

Once the connection was fixed, DIC results were visualised using contour plots, which provided detailed strain distribution and vertical displacement data, confirming the FEA results in Fig. 6, that the vertical displacement of the specimen was minimal, and that deformation of the arms is symmetrical, indicating that the design changes were successful in mitigating unwanted mode coupling (Fig. 8). Comparing LASER vs DIC results yielded negligible differences of up to 5% (equivalent to about 1 µm, which is in the range of the accuracy of the LASER being used).

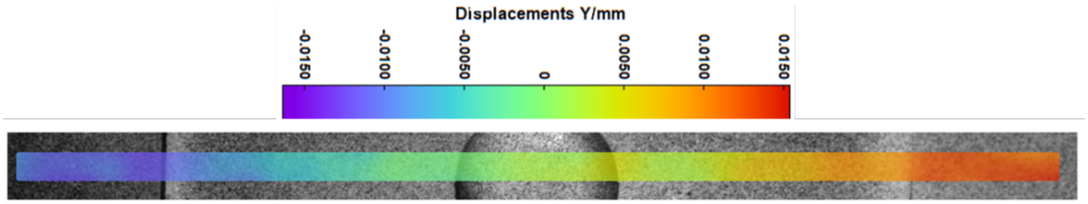

Fig. 8. DIC countor plot of the displacement across one arm of the specimen.

The strain measurements at the centre of the specimen, obtained using DIC, were compared with the tip displacements measured by point LASERs (Fig. 9), showing strong agreement. This confirmed strain uniformity across the specimen during testing.

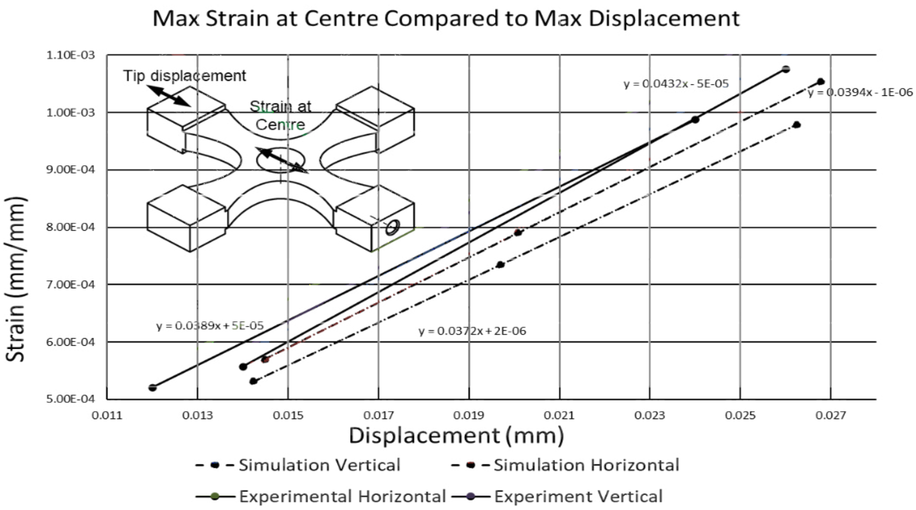

Fig. 9. Maximum strain at centre compared to maximum displacement at tip.

Finally, it is worth noting that a total of five different specimens were tested in this study. The majority of the results focus on one particular specimen, as the first four specimens (with measured overall lengths of 105.2 mm) showed non-unitary biaxiality ratios of approximately 0.71. The horn and booster stack used had a natural frequency of 20.32 kHz, but with the initial specimens, this frequency dropped to around 20.15 kHz. Based on coupling principles in Modal Analysis (Maia and Silva, 1997), it is reasonable to assume that the differing natural frequencies between the stack and specimen caused mode coupling, resulting in the unintended non-unitary biaxiality ratios (effectively, it resulted in a new system with new mode shapes, however similar). To address this, the specimens were fine-tuned by trimming 1.5 mm from each side, leading to a system frequency (stack + specimen) of 20.30 kHz and an improved biaxiality ratio of 0.92. Although this was not further refined to achieve a unitary biaxiality ratio, as this outcome is anticipated by those with experience in Modal Analysis, it remains essential to design the stack and specimens (whether uniaxial or multiaxial) to resonate as closely as possible.

5. Conclusions

The aim of this work was to develop and validate a novel cruciform specimen design for Ultrasonic Fatigue Testing (UFT) to overcome the longstanding issue of interference from non-desired modes, particularly the flexural 'flapping mode.' This interference has previously undermined the accuracy of biaxial testing, making it challenging to achieve reliable results across the full range of biaxiality ratios. The significance of this work lies in its successful practical realisation of a solution to this problem, enabling precise, in-phase biaxial UFT, which was previously considered largely theoretical in its practical application with equibiaxial cruciform specimens of the type used in this study.

In conclusion, this study has introduced an innovative design that effectively separates the axial and interfering modes, minimising mode coupling and ensuring that testing results are accurate and reliable. Through Finite Element Analysis (FEA) and Digital Image Correlation (DIC), the geometry was optimised, and the results were experimentally validated. Moreover, careful attention was given to reducing transient modes through improved connection methods, such as the use of beeswax between the horn and specimen and optimised threading techniques.

The research also emphasises the importance of multi-objective optimisation, considering both minimising mode coupling and reducing stress concentrations at critical points, which should be the subject of attention for future work. Finally, the insights gained from this work have the potential to inform more accurate fatigue life prediction models, making a significant contribution to the future of accelerated fatigue testing. These innovations mark a substantial advance in the field, offering practical solutions that enhance the capabilities of UFT for biaxial testing in high-cycle fatigue regimes.

Acknowledgements

The authors acknowledge Fundação para a Ciência e a Tecnologia (FCT, Portugal) for its financial support via the project LAETA Base Funding (DOI: 10.54499/UIDB/50022/2020), and Research England (United Kingdom), through the ADDISONIC's Bournemouth University Strategic Investment Area.

References

Bathias, C., 1999. There is no infinite fatigue life in metallic materials. Fatigue & Fracture of Engineering Materials & Structures 22, 559–566.

Baptista, R.; Claudio, R.; Reis, L.; Madeira, J.; Guelho, I.; Freitas, M., 2015. Optimization of cruciform specimens for biaxial fatigue loading with direct multi search. Theoretical and Applied Fracture Mechanics 80, 65–72.

Costa, P.; Montalvão, D.; Freitas, M.; Baxter, R.; Reis, L., 2019. Cruciform specimens' experimental analysis in ultrasonic fatigue testing. Fatigue & Fracture of Engineering Materials & Structures 42, 2496–2508.

Costa, P, Nwawe, R, Soares, H, Reis, L, Freitas, M, Chen, Y, Montalvão, D., 2020. Review of multiaxial testing for very high cycle fatigue: From "Conventional" to ultrasonic machines. Machines 8(2), 25.

Freitas, M., 2017. Multiaxial fatigue: From materials testing to life prediction. Theoretical and Applied Fracture Mechanics 92, 360–372.

Furuya, Y., Shimamura, Y., Takanashi, M., Ogawa, T., 2022. Standardization of an ultrasonic fatigue testing method in Japan. Fatigue & Fracture of Engineering Materials & Structures 45, 2415-2420.

Maia, N., Silva, J., 1997. Theoretical and experimental modal analysis. Research Studies Press Taunton, Somerset, England.

Montalvão, D.; Wren, A., 2017. Redesigning axial-axial (biaxial) cruciform specimens for very high cycle fatigue ultrasonic testing machines. Heliyon 3(11), e00466.

Montalvão, D.; Blaskovics, A.; Costa, P.; Reis, L.; Freitas, M., 2019. Numerical analysis of VHCF cruciform test specimens with non-unitary biaxiality ratios. International Journal of Computational Methods and Experimental Measurements 7, 327–339.